Synthesis of Zinc Silicate Using Silica from Rice Hull Ash (RHA) Through Solid-State Reaction

Tender PANGILINAN-FEROLIN
Ateneo de Davao University , Davao City, Philippines
tpferolin@addu.edu.ph

Reynaldo M. VEQUIZO
Mindanao State University-Iligan Institute of Technology, Iligan City, Philippines
vequizorey2@gmail.com

ABSTRACT

Successful synthesis of nanocrystalline Zn_2SiO_4 powders using solid state reaction of the ZnO powder precipitate and amorphous cristobalite SiO_2 powders from processed rice hull ash at $800 \leq T \leq 1000^oC$ is presented in this study. ZnO powders were grown by chemically reacting stoichiometric NaOH and $ZnSO_4$. The solid state reacted powders were characterized using scanning electron microscopy (SEM) with energy dispersive x-ray spectroscopy (EDX), Fourier transform spectroscopy (FTIR) and x-ray diffraction (XRD). Microscopic analyses of the annealed powders were consistent with reported morphological structures of Zn_2SiO_4. FTIR results indicate the presence of ZnO_4 and SiO_4 groups corresponding to Zn_2SiO_4. XRD results further revealed that Zn_2SiO_4 powders were synthesized at the reaction temperatures of 900 and 1000^oC with onset growth at 800^oC. The method used in this study shows that Zn_2SiO_4 can be grown at a much lower temperature ($800 \leq T \leq 1000^oC$) compared to the reported temperature of synthesizing Zn_2SiO_4 through solid-state reaction. The Zn_2SiO_4 powders exhibit dominant a-axis orientation and the average crystallite size for zinc silicate powders annealed at 1000^oC is about 33 nm. The results suggest that the Zn_2SiO_4 powders are promising materials for phosphor applications. Using SiO_2 from RHA in the synthesis of $ZnSiO_4$ increases the value of rice hulls and as a result becomes beneficial to rice farmers and that RHA collection and utilization policies has to be incorporated in local governments.

Keywords: *$ZnSiO_2$, SiO_2, amorphous, solid-state reaction*

INTRODUCTION

Doped zinc silicate (Zn_2SiO_4) is utilized in various electronic applications such as cathode ray tubes (Jiang, Chen, Xie, & Zheng, 2010), plasma display panels (Takesue, Suinob, Hakutab, Hayashib, & Smith, 2010), electroluminescent equipment (Zeng, Fu, Lou, Yu, Sun, & Li, 2009) and imaging devices for

mammographic applications (Lou, et al., 2007). Zn_2SiO_4 is used as host matrix for doping ions such as europium (Eu^{3+}), terbium (Tb^{3+}), nickel (Ni^{2+}) and manganese (Mn^{2+}) (Inoue, Toyoda, & Morimoto, 2008; El Mir, 2007; Mai, Feldmann, & Claus, 2009). However, despite the importance of zinc silicate in electronics industry, the Philippines is unable to produce zinc silicate that can largely attribute to the following: (1) the existing processes used in the synthesis of zinc silicate powders requires acquisition of modern and expensive equipment, (2) the present methods used require high working temperatures between 1200 and 3250^{o}C, and (3) the technique used in the synthesis of zinc silicate requires chemical reagents which have working conditions that are uneconomical in tropical countries, expensive and need to be imported. Thus, with the current economic and energy crisis that the country is experiencing, it is imperative to explore other process of synthesis addressing the concerns cited. Hence, this study is undertaken to synthesize zinc silicate using locally available precursors, readily available equipment, lower temperature requirement for synthesis and manufacture of high-grade zinc silicate in the country that can be utilized for significant uses in the electronics industry.

The current production of zinc silicate utilizes inorganic precursors such as zinc oxide (Lukić, Petrovic´, Dramićanin, Mitric´, & Đacˇanin, 2008), $Zn(NO_3)_2$ (Alavi, Dexpert-Ghys, & Caussat, 2008) and $Zn(OOCCH_3)_2$ (Sharma & Bhatti, 2009) as Zn source and tetraethylorthosilicate (TEOS) (El Mir, 2007; Lukić, Petrovic´, Dramićanin, Mitric´, & Đacˇanin, 2008), quartz SiO_2 (Xu, et al., 2004) and hexamethyldisoloxane (HMDSO) (Tani, Takatori, & Pratsinis, 2004) as source for SiO_2. Zinc acetate, on the other hand, is usually used as the precursor source of zinc (Tani, Takatori, & Pratsinis, 2004), (Tani, Watanabe, & Takatori, 2003; Zeng, Fu, Lou, Yu, Sun, & Li, 2009). Other methods make use of zinc oxide and silicon dioxide powders as the precursors (Inoue, Toyoda, & Morimoto, 2008). However, the precursors used such as TEOS and HMDSO have unfavorable characteristics. For instance, TEOS has a flash point of 52^{o}C (Jang, 1999). Its use is a setback in tropical countries like the Philippines where ambient temperature is 33^{o}C but can be higher during summer months. On the other hand, HMDSO has an even lower flash point of -3^{o}C (Catoire & Naudet, 2004). Thus, the working temperature must be much lower than -3^{o}C. Maintaining such condition is impractical for countries like the Philippines. On the other hand, researches on the synthesis of SiO_2 from RHA had been explored (Le, Thuc, & Thuc, 2013). However, utilizing SiO_2 from RHA in the production of nanocrystalline Zn_2SiO_4 has yet to be investigated.

Zinc silicate is usually prepared using flame spray pyrolysis, emulsion combustion method, sol-gel process, evacuated sealed silica tube method, chemical vapor deposition route, solid-state reaction and hydrothermal condition to name a few. The method of synthesis relied on the nature of the expected final form of zinc silicate. Most of the above processes involved nitrogen atmosphere or controlled pure oxygen supply. Furthermore, these processes, except for sol-gel and hydrothermal methods, require high temperature conditions between 1200 and 3250^{o}C (Tani, Takatori, & Pratsinis, 2004; Tani, Watanabe, & Takatori, 2003; Inoue, Toyoda, & Morimoto, 2008; Selomulya, Ski, Pita, Kam, Zhang, &

Buddhudu, 2003; Lee & Lua, 2000; Xu, O'Keefe, & Perry, 2004; Zhang, et al., 2001; El Mir, Amlouk, Barthou, & Alaya, 2007; Xu, Xu, Zheng, & Wu, 2010; Natarajan, V., Murthy, & Kumar, 2005).

Existing studies are unable to explore the use of SiO_2 obtained from rice hull ash (RHA) in the synthesis of Zn_2SiO_4 that can contribute to the commercial availability of SiO_2 from processed RHA. Thus, the use of amorphous cristobalite SiO_2 from processed RHA can be considered as a viable precursor for Zn_2SiO_4. Moreover, the production of ZnO as coating from NaOH and $ZnSO_4$ is also unexplored in the synthesis of Zn_2SiO_4. Hence, this study utilizes the use of amorphous cristobalite SiO_2 from processed RHA and ZnO produced from NaOH and $ZnSO_4$. In addition, despite of the fact that this paper is technical in nature, its results on the use of agricultural waste such as rice hull ash (RHA), when processed and used for various electronic application, has increased its economic value. This, as a result, becomes beneficial to innovators, phosphor and electronic industries, and of course, to rice farmers. In this manner, local government units can come up policies related to collection and utilization of RHA as one of its value-added products.

METHODOLOGY

Zinc silicate (Zn_2SiO_4) is synthesized using equimolar concentrations of zinc sulfate ($ZnSO_4$) and sodium hydroxide (NaOH) producing zinc hydroxide ($Zn(OH)_2$). The addition of strong electrolyte ($ZnSO_4$) and strong base (NaOH) in an aqueous solution results to the exchange of ions. The formation $Zn(OH)_2$ and Na_2SO_4 is the product of ion exchange. $Zn(OH)_2$ is insoluble in water thus it remains as solid in an aqueous solution. On the other hand, Na_2SO_4 is soluble in water hence it is in liquid phase. The reaction proceeds as follows

$$ZnSO_4(aq) + 2NaOH(aq) \xrightarrow{heat, 80^o C} Zn(OH)_2(s) + Na_2SO_4(l).$$

The resulting solution is filtered and washed with distilled water. The precipitate is mixed with appropriate amount of silicon dioxide (SiO_2) in water with constant stirring at an elevated temperature of 80°C. Neither $Zn(OH)_2$ and SiO_2 are soluble in water. Thus, no chemical reaction is expected in the mixing of $Zn(OH)_2$ and SiO_2. However, the water is used as an amalgamation medium to promote the adhesion of $Zn(OH)_2$ particles on the surface of SiO_2 creating a nucleation site where $Zn(OH)_2$ particles coat SiO_2. The reaction mechanism for this process is

$$Zn(OH)_2(s) + SiO_2(s) \xrightarrow{heat, 80^o C} Zn(OH)_2(s) + SiO_2(s) + H_2O(g).$$

The precipitate is washed with distilled water and dried at 100°C. The dried precipitate is annealed at 800, 900 and 1000°C. Solid-solid diffusion is expected to occur at these temperatures. The mixing stage promote the adhesion of smaller particle $Zn(OH)_2$ to the surface of SiO_2 allowing the formation of Zn_2SiO_4 at

lower temperature. Thus, the powders annealed at $800 \leq T \leq 1000^oC$ are expected to contain Zn_2SiO_4 following the process

$$2\ Zn(OH)_2(s) + SiO_2(s) \xrightarrow{\textit{heat}, 800–1000^oC} Zn_2SiO_4 + H_2O\ (g).$$

The resulting powders are characterized using scanning electron microscopy (SEM) equipped with energy dispersive x-ray spectroscopy (EDX), Fourier transform infrared spectroscopy (FTIR) and x-ray diffraction (XRD). The SEM micrographs are obtained with voltage operating condition of 20 kV. The samples are magnified to 150, 500 and 2000x with scales corresponding to 100, 50 and 10μm, respectively. The energy dispersive x-ray (EDX) operating conditions in obtaining elemental analysis using EDX are 10 keV at 500x magnification. In the Fourier transform infrared (FTIR) spectroscopy, the KBr powders are used as standard and the scan range from 450 to 4000 cm^{-1}. The XRD characterization of the annealed powder samples is done using CuKα x-ray source and scans from 10 to 70^o at an increment of 0.02^o/0.6 second.

RESULTS AND DISCUSSIONS

Scanning Electron Microscopy (SEM)

The SiO_2 produced from RHA is generally made up of large particles as shown in Figure 1. The micrograph also indicated hollow regions that can be penetrated by $Zn(OH)_2$ particles during mixing of $Zn(OH)_2$ and SiO_2 using water as medium. Hence, increasing the contact surfaces between $Zn(OH)_2$ and SiO_2 intensifies the formation of Zn_2SiO_4 at lower temperature.

SEM micrographs of Zn_2SiO_4 annealed at $800 \leq T \leq 1000^oC$ are similar to the reported morphology of zinc silicate prepared using solid-state reaction (Takesue, Hayashi, & Smith, 2009). The micrograph of Zn_2SiO_4 annealed at 800^oC show coalesced flake-like mass which is only present at this temperature. This morphology is unreported and needs to be explored further regarding its composition. However, it can be deduced that as the annealing temperature increases the dimension of Zn_2SiO_4 gets smaller and the structure becomes more defined. Moreover, the XRD results show that Zn_2SiO_4 has indeed started to grow at 800^oC which is further confirmed in the FTIR spectra. Thus, it can be said that flaky materials may be SiO_2 and ZnO in solid-solid diffusion phase and less likely to be the synthesized Zn_2SiO_4. As observed, the size of Zn_2SiO_4annealed at 1000^oC is smaller in size compared to Zn_2SiO_4 powders annealed at 900^oC as shown in Figure 2.
Hence, confirming the successful synthesis of Zn_2SiO_4 using NaOH, $ZnSO_4$ and amorphous cristobalite SiO_2 obtained from processed RHA through annealing. However, the large particles observed at 1000^oC are agglomeration of Zn_2SiO_4

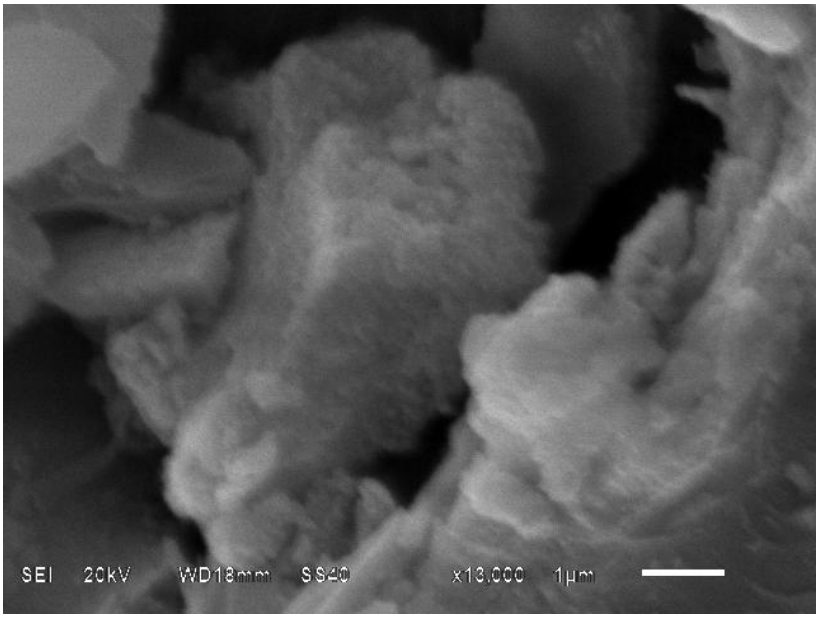

Figure 1. SEM micrograph of the amorphous cristobalite SiO_2.

To verify whether this morphology changes with the addition of amorphous cristobalite silicon dioxide from rice hull ash, a sequential analysis of the as grown powders with silica is done.

The SEM micrograph of the zinc hydroxide powder shown in Figure 2, displays that large particles are encased by flakes suggesting that zinc hydroxide has probably decomposed to zinc oxide during fusing at 80^oC. This conversion from zinc hydroxide to zinc oxide is confirmed by Fourier transform infrared spectroscopy that can be found in the succeeding section. Elemental analysis reveals that the powder is made up of zinc and oxygen which implies that the composition of the sample is zinc hydroxide and probably zinc oxide as well. However, the amount of zinc and oxygen are almost equal. This suggests that the amount of oxygen present is insufficient to form zinc hydroxide considering that the ratio of oxygen and zinc is 2:1, thus confirming the decomposition of zinc hydroxide to zinc oxide.

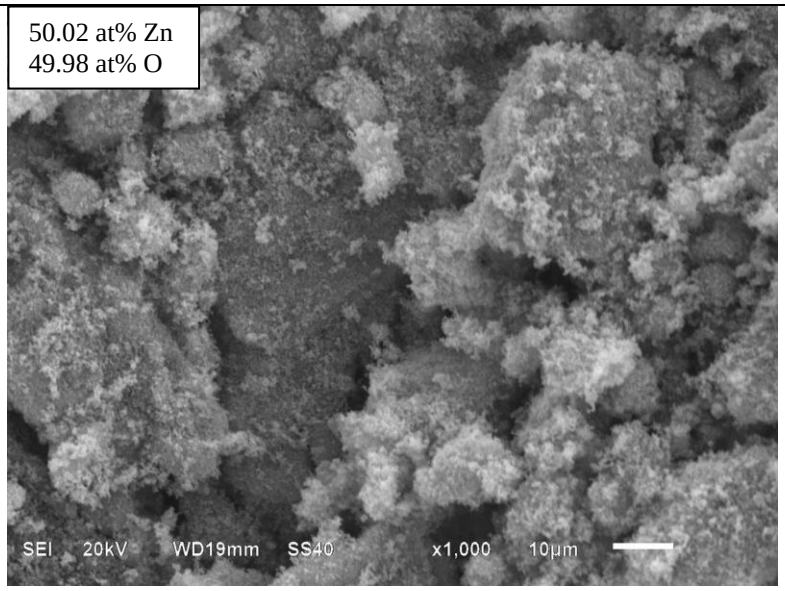

Figure 2. SEM micrograph of zinc hydroxide powders.

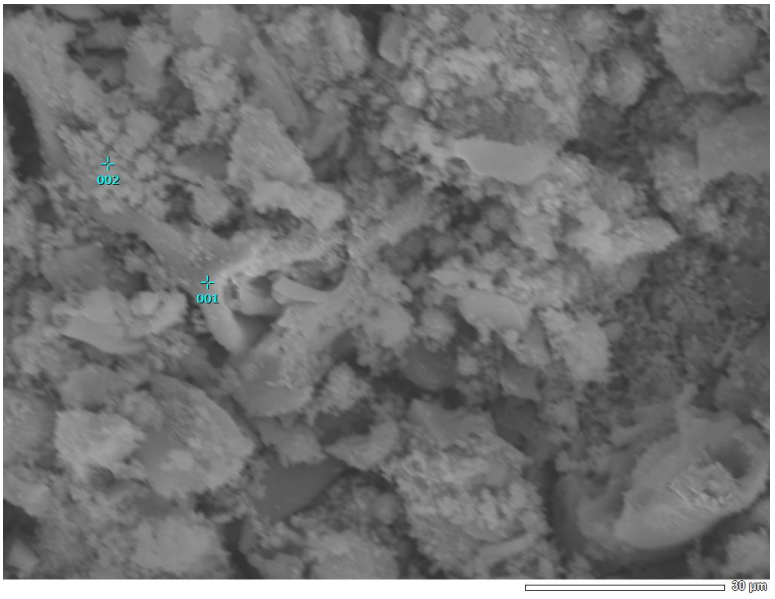

Figure 3. Sequential images of as grown powders $Zn(OH)_2$+SiO_2.

The SEM micrograph in Figure 3 is used for the sequential scanning to identify the composition of these materials. These show that the larger particles mostly consist of silicon and oxygen (point 001) and the flakes are largely made up of zinc and oxygen (point 002). Large particles marked as point 001 of the as grown preparations shown in Figure 3 display that it mainly contains silicon. This

suggests that the large particles are primarily amorphous cristobalite silicon dioxide. On the other hand, point 002 marking the flakes indicates that it mostly contains zinc and oxygen, implying that this may be made up of zinc hydroxide. However, micrograph and elemental analysis shown in Figure 2 revealed that mixing zinc sulfate and sodium hydroxide at 80°C has formed both zinc hydroxide and zinc oxide. Thus, the combination of mixing and additional heating during the fusing phase of zinc hydroxide/zinc oxide with amorphous cristobalite silicon dioxide, may have induced the decomposition of the remaining zinc hydroxide to zinc oxide. Therefore, zinc hydroxide has completely decomposed to zinc oxide during the mixing phase at an elevated temperature of 80°C.

This is verified using FTIR which is discussed in the succeeding section. Microscopic analyses of as grown powders show that these have similar morphological structures. Comparing the morphological structure of zinc hydroxide/zinc oxide shown in Figure 3, the micrograph shows evidence that zinc hydroxide/zinc oxide coated the large-particle amorphous silicon dioxide. The adhesion of zinc hydroxide/zinc oxide to the surface of amorphous silicon dioxide includes its infusion into the crevices of silicon dioxide. Thus, it is possible that $Zn(OH)_2/ZnO$ has substantially covered the surface of the amorphous silicon dioxide. The initial contact between these materials allows better amalgamation of zinc hydroxide and silicon dioxide to form zinc silicate even at low temperature.

The mechanism of zinc hydroxide/zinc oxide coating on the surface of amorphous cristobalite silicon dioxide is shown on Figure 4.

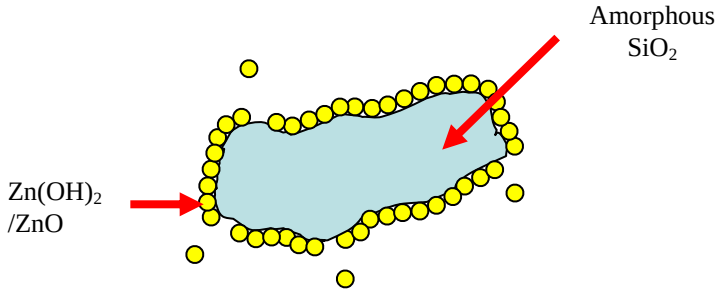

Figure 4. Coating mechanism of amorphous cristobalite silicon dioxide with zinc hydroxide/zinc oxide and manganese hydroxide.

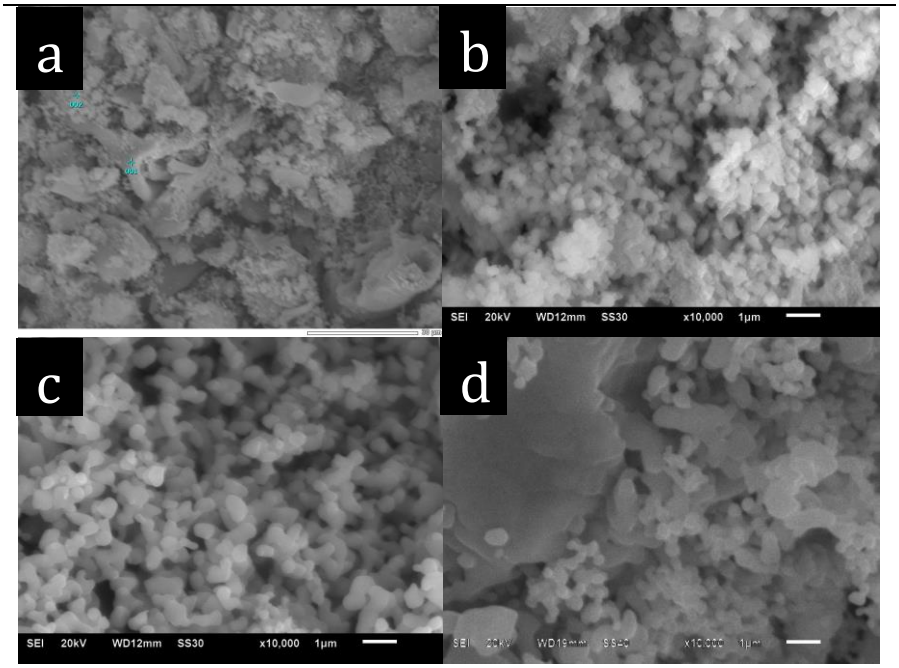

Figure 5. Micrographs of $Zn(OH)_2/ZnO + SiO_2$ (a) as grown and powders annealed at (b) 800°C (c) 900°C and (d) 1000°C.

The coating of amorphous cristobalite silicon dioxide with zinc hydroxide/zinc oxide during fusing stage may have induced the growth of zinc silicate even at 80°C. FTIR spectra of the as grown powders confirm that the formation of amorphous zinc silicate has indeed occurred during mixing at 80°C. The discussion on the FTIR spectra of as grown powders is discussed in detail in the succeeding section.

Fourier Transform Infrared Spectroscopy (FTIR)

The FTIR spectra shown in Figure 6 of as grown powders show dominant peaks between 460 to 1242 cm^{-1}. Vibrational mode at 472 cm^{-1} which corresponds to ZnO stretching is more defined as the concentration of manganese increases. Thus, the presence of this stretching suggests that as grown powders already contain zinc oxide. As shown in Figure 2, the morphology of zinc hydroxide contains more than one structure which implies that probably zinc oxide has indeed formed at 80°C. The elemental analysis of zinc hydroxide also suggests such conversion and this is confirmed by the FTIR spectra where ZnO stretching is measured. The vibrational mode at 578 cm^{-1} refers to ZnO_4 symmetric stretching. The presence of ZnO_4 and SiO_4 in the FTIR spectra indicates the formation of zinc silicate. Thus, it is verified that at 80°C amorphous zinc silicate has been formed already.

On the other hand, peaks at 798 and 1091 cm^{-1} indicate shifted Si−O−Si vibration and Si–O asymmetric stretching, respectively. These vibrations are ascribed to the presence of loosely bound silicon oxides (Chakradhar, Nagabhushana, Chandrappa, Ramesh, & Rao, 2004; Yan, Ji, Xi, Wang, Du, & Zhao, 2006; Ying-Mei, et al., 2010). Thus from these results, zinc silicate powders are annealed and analyzed.

Zn_2SiO_4 powders annealed at $800 \leq T \leq 1000^oC$ are further characterized using FTIR. The presence of peaks representing ZnO_4 and SiO_4 groups indicate the growth of Zn_2SiO_4. Based on previous studies of Zn_2SiO_4 synthesized using solid-state reaction, annealing temperature must be between 1100 and 1400^oC to produce zinc silicate (Takesue, Hayashi, & Smith, 2009). However, FTIR spectra of the synthesized zinc silicate powders annealed at 800^oC show that vibration corresponding to ZnO_4 and SiO_4 measured at 578 and 904 $cm^{-1,}$ respectively, is already observed as shown in Figure 3. This vibration specifies the growth of Zn_2SiO_4 at this temperature which is also confirmed in the XRD. The growth of Zn_2SiO_4 at 800^oC is, to a large extent, lower than the reported annealing temperature for solid-state reaction to produce Zn_2SiO_4. Moreover, FTIR spectra of the synthesized Zn_2SiO_4 show that powders annealed at 900 and 1000^oC exhibit symmetric and asymmetric stretching and deformation vibration modes of ZnO_4 and SiO_4 as observed in Figure 3. These indicate that Zn_2SiO_4 is synthesized at these temperatures. The SiO_4 asymmetric stretching vibration mode are at 934 and 978 cm^{-1}. Zn_2SiO_4 powders annealed at 900 and 1000^oC exhibited all wavelengths corresponding to SiO_4 asymmetric stretching (Sharma & Bhatti, 2009; Zeng, Fu, Lou, Yu, Sun, & Li, 2009; Yan, Ji, Xi, Wang, Du, & Zhao, 2006).

Thus, FTIR spectra of Zn_2SiO_4 powders annealed at 900 and 1000^oC have shown all wavenumbers pointing to ZnO_4 and SiO_4 of Zn_2SiO_4 indicating that Zn_2SiO_4 powders are produced at these temperatures. ZnO vibration measured at 472 cm^{-1} indicative that ZnO is produced even at 80^oC. Moreover, FTIR spectra of the as grown powders, prepared by mixing $ZnSO_4$ and NaOH to produce $Zn(OH)_2$, show that ZnO_4 vibration measured at 578 cm^{-1} is recorded indicating that amorphous Zn_2SiO_4 has been produced (Sharma & Bhatti, 2009). This reiterates that using amorphous SiO_2 is a preferred structure for the synthesis of Zn_2SiO_4 because this allows $Zn(OH)_2$/ZnO to adhere to more surface area of SiO_2 thus requiring lower temperature to form Zn_2SiO_4. This is confirmed in the XRD results of Zn_2SiO_4 powders annealed between $800 \leq T \leq 1000^oC$.

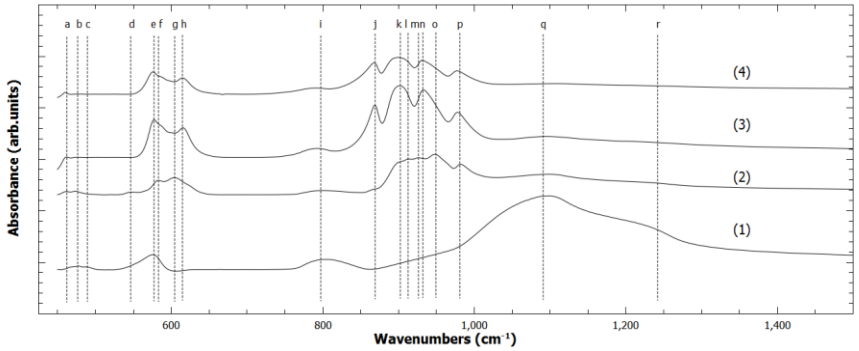

Figure 6. FTIR spectra of $Zn(OH)_2$/ZnO + SiO_2 (1) as grown at 80°C and powders annealed at (2) 800°C (3) 900°C (4) 1000°C. The wavenumbers recorded are (a) 460 (b) 462 (c) 472 (d) 547 (e) 573 (f) 578 (g) 605 (h) 615 (i) 798 (j) 867 (k) 904 (l) 913 (m) 927 (n) 934 (o) 950 (p) 978 (q) 1091 (r) 1242 cm^{-1}.

X-ray Diffraction (XRD)

XRD reveals that Zn_2SiO_4 is synthesized at annealing temperatures of 900 and 1000°C with onset growth at 800°C. XRD patterns of Zn_2SiO_4 annealed at these temperatures show diffraction peaks measured at $2\theta \approx 12.26$, 21.46, 25.15, 31.15, 33.6, 38.45, 44.67, 48.57, and 68.36° attributed to Zn_2SiO_4 (willemite-zinc silicate, JCPDS# 37-1485). Furthermore, the XRD patterns show that ZnO is already formed at 400°C which indicate that the $Zn(OH)_2$ produced in the reaction of NaOH and $ZnSO_4$ has been completely converted to ZnO. Peaks indicating the presence of ZnO are $2\theta \approx 31.42$, 34.13, 35.93, 47.25, 56.29 and 62.61° for zincite-zinc oxide, JCPDS# 36-1451. The presence of these peaks is due to the partial amalgamation of ZnO and amorphous cristobalite SiO_2 to form Zn_2SiO_4. At 800°C, peaks around $2\theta \approx 21.53$, 25.11, 31.4 and 44.52° indicate that Zn_2SiO_4 is synthesized at this temperature together with other phases of ZnO and SiO_2. Moreover, the XRD results shows that the composition of the Zn_2SiO_4 powders annealed at 900 and 1000°C mainly consist of crystalline Zn_2SiO_4. This emphasizes that the synthesis of Zn_2SiO_4 is achieved at 1000°C.

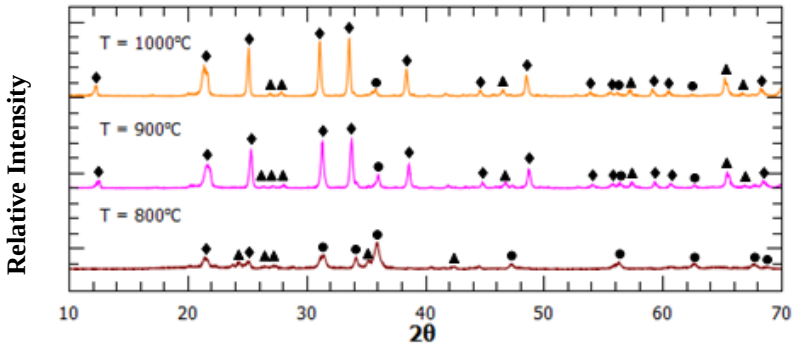

Figure 7. XRD patterns of zinc silicate annealed at 800, 900 and 1000°C. Legend: ♦ - Zn_2SiO_4, ● - ZnO and ▲ - SiO_2.

which is lower than the reported temperature for solid-state reaction to produce zinc silicate (Takesue, Hayashi, & Smith, 2009). Thus, increasing the annealing temperature and soaking time may induce the complete conversion of the unreacted zinc oxide and silicon dioxide. However, the possibility of producing a different compound is plausible and need to be explored further. The highest relative intensity for the synthesized Zn_2SiO_4 annealed at $800 \leq T \leq 1000^oC$ is observed at $2\theta \approx 25.18$, 31.14 and 44.67^o. These indicate that the preferred orientations of the synthesized Zn_2SiO_4 are (220), (113) and (410) (willemite-zinc silicate, JCPDS# 37-1485).

The XRD results as shown in Figure 7 reveal that only small amounts of zinc oxide and silicon dioxide remained unreacted at 1000°C. Substantially, all peaks indicate the presence of zinc silicate. The analysis of the XRD patterns indicates that the peaks in the XRD of synthesized zinc silicate broadened compared to the peaks of the standard zinc silicate (willemite-zinc silicate, JCPDS #37-1485). This deviation can be due to either particle size or strain broadening (Williamson & Hall, 1953). According to Stokes and Wilson, the particle size and strain can be determined by

$$\frac{\beta \cos\theta}{\lambda} = \xi\left(\frac{2\sin\theta}{\lambda}\right) + \frac{1}{t},$$

where β is the full width half maximum (FWHM), in radians, ξ is the strain, λ is the wavelength of CuKα, θ is half of the dominant diffraction angle and t is the mean particle diameter. From this equation, the slope $\xi > 0$ indicates tension and $\xi < 0$ denotes compression (Tabor, 2000). To determine the cause of deviation between the peaks of the synthesized zinc silicate and the standard zinc silicate a graph of $\frac{\beta\cos\theta}{\lambda}$ vs. $\frac{2\sin\theta}{\lambda}$ is plotted. The condition of synthesis, which is of interest in the determination of the cause of broadening, are the powders prepared at 900 and 1000°C. These temperatures, based on the FTIR spectra and XRD, exhibit the most amount of synthesized zinc silicate.

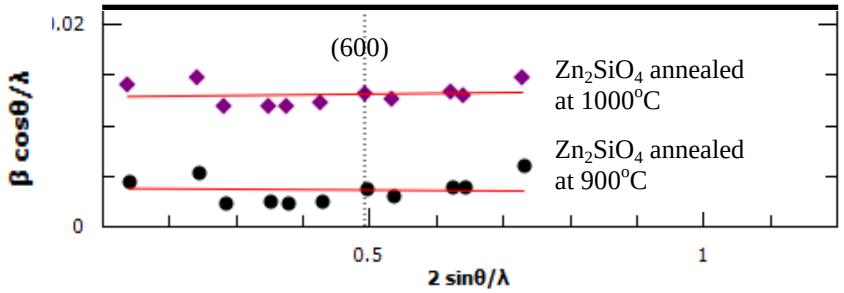

Figure 8. A graph on the broadening due to particle size and strain.

Figure 8 shows that the crystallite of (600) plane shows that it is closest to the fitted line and holds true for all synthesized zinc silicate at this orientation. Thus, it confirms that the synthesized zinc silicate is a-axis oriented dominantly as reiterated in the highest peaks shown in the XRD patterns pointing to (220), (113) and (410) as preferred orientations (willemite-zinc silicate, JCPDS # 37-1485). The average crystallite size for zinc silicate powders annealed at 900°C and 1000°C is about 33 nm. Previous study reported average crystallite size of 145 nm (Selomulya, Ski, Pita, Kam, Zhang, & Buddhudu, 2003). This suggests that the method used in this research is able to obtain a smaller average crystallite size of zinc silicate. The fabrication of nanocrystalline Zn_2SiO_4 shows promising application as phosphor (Alavi, Dexpert-Ghys, & Caussat, 2008).

Societal Implications of the Results

From the results, we have indeed produced Zn_2SiO_4 powders from the mixture of SiO_2 from processed rice hull ash (RHA) and ZnO complexes with subsequent annealing for solid-state reaction to occur. The local government, the community innovators, the rice farmers and the phosphor industries can therefore consider these results for the production of Zn_2SiO_4 powders with SiO_2 derived from RHA as additional value-added products. The local government can, for instance, come up with policies on RHA collection for such utilization and start collaborative efforts with phosphor industries in the production of quality Zn_2SiO_4 powders for phosphor application and possible commercialization. In this manner, the local government, the community farmers and innovators and the phosphor industries will increase and strengthen their intellectual property (IP) portfolio.

CONCLUSION

Nanocrystalline Zn_2SiO_4 powders were successfully synthesized using NaOH, $ZnSO_4$ and amorphous cristobalite SiO_2 from processed RHA and subsequent annealing for solid state reaction to occur. Furthermore, ZnO and amorphous

Zn_2SiO_4 are produced at 80°C. Microscopic analyses of annealed powders at $800 \leq T \leq 1000$°C were consistent with reported morphological structures of Zn_2SiO_4. This was verified by the FTIR spectra which indicate the presence of peaks representing ZnO_4 and SiO_4 groups signifying the presence of Zn_2SiO_4. XRD revealed further that Zn_2SiO_4 is synthesized at annealing temperatures of 900 and 1000°C with onset growth at 800°C. The method used in this study shows that Zn_2SiO_4 can be produced at a much lower temperature ($800 \leq T \leq 1000$°C) compared to the reported temperature of synthesizing Zn_2SiO_4 through solid-state reaction. Based on full width half maximum (FWHM) and diffraction angle, the synthesized Zn_2SiO_4 is a-axis oriented dominantly as reiterated in the highest peaks shown in the XRD patterns pointing to (220), (113) and (410) as preferred orientations. Moreover, the average crystallite size for zinc silicate powders annealed at 1000°C is about 33 nm, an indication that it is a promising material for phosphor applications. In addition, the findings in this study suggest some policy related issues on the value-added utilization of RHA in the production of Zn_2SiO_4 powders in the local government units.

ACKNOWLEDGEMENT

The researchers would to thank DOST-PCIEERD for the scholarship grant, the equipment used in this study in the Materials Science Laboratory of the Physics Department of MSU-Iligan Institute of Technology and John Paul Aseniero for the amorphous silica used in this study. Utmost gratitude to Ateneo de Davao University President Fr. Joel E. Tabora, S.J., Academic Vice-President Fr. Gabriel Jose T. Gonzalez, S.J. and School of Engineering and Architecture Dean Dr. Randell U. Espina for their support through the University Research Council (URC) headed by Ms. Lourdesita Sobrevega-Chan.

REFERENCES

Alavi, S., Dexpert-Ghys, J., & Caussat, B. (2008). High temperature annealing of micrometric Zn_2SiO_4:Mn phosphor powders in fluidized bed. Materials Research Bulletin, 43, 2751-2762

Catoire, L. & Naudet, V. (2004), A Unique Equation to Estimate Flash Points of Selected Pure Liquids Application to the Correction of Probably Erroneous Flash Point Values. Journal of Physical and Chemical Reference Data, 33, 1083-1111

Chakradhar, R. S., Nagabhushana, B. M., Chandrappa, G. T., Ramesh, K. P., & Rao, J. L. (2004). Solution combustion derived nanocrystalline Zn_2SiO_4:Mn phosphors: A spectroscopic view. Journal of Chemical Physics, 121, 10250-10259

El Mir, L., Amlouk, A., Barthou, C., & Alaya, S. (2007). Synthesis and luminescence properties of $ZnO/Zn_2SiO_4/SiO_2$ composite based on nanosized zinc oxide-confined silica aerogels. Physica B: Condensed Matter, 68, 412-417

Inoue, Y., Toyoda, T., & Morimoto, J. (2008). Photoacoustic spectra on Mn-doped zinc silicate powders by evacuated sealed silica tube method. Journal of Materials Science, 43, 378-383

Jang, H.D. (1999). Generation of Silica Nanoparticles from Tetraethylorthosilicate (TEOS) Vapor in a Diffusion Flame. Aerosol Science and Technology, 30, 477-488

Jiang, Y., Chen, J., Xie, Z., & Zheng, L. (2010). Syntheses and optical properties of α- and β-Zn_2SiO_4: Mn nanoparticles by solvothermal method in ethylene glycol-water system. Materials Chemistry and Physics, 120, 313-318

Le, V. H., Thuc, C. N. H., & Thuc, H. A. (2013). Synthesis of silica nanoparticles from Vietnamese rice husk by sol-gel method. Nanoscale Research Letters, 8(1), 58

Lee, B. I., & Lua, S. W. (2000). Synthesis of nanoparticles via surface modification for electronic applications. Journal of Ceramic Processing Research, 1 (1), 20-26

Lou, T. J., Zeng, J. H., Lou, X. D., Fu, H. L., Wang, Y. F., Ma, R. L., et al. (2007). A facile synthesis to Zn_2SiO_4:Mn^{2+} phosphor with controllable size and morphology at low temperature. Journal of Colloid and Interface Science, 314, 510-513

Lukić, S., Petrovic´, D., Dramićanin, M., Mitric´, M., & Đacˇanin, L. (2008). Optical and structural properties of Zn_2SiO_4:Mn^{2+} green phosphor nanoparticles obtained by a polymer-assisted sol-gel method. Scripta Materiala, 58, 655-658.

Mai, M., Feldmann, & Claus. (2009). Two-color emission of Zn_2SiO_4:Mn from ionic liquid mediated synthesis. Solid State Sciences, 11, 528-532

Natarajan, V., Murthy, K., & Kumar, M. J. (2005). Photoluminescence investigations of Zn_2SiO_4 co-doped with Eu^{3+} and Tb^{3+} ions. Solid State Communications, 134, 261-264

Selomulya, R., Ski, S., Pita, K., Kam, C., Zhang, Q., & Buddhudu, S. (2003). Luminescence properties of Zn_2SiO_4:Mn^{2+} thin-films by a sol-gel process. Materials Science and Engineering, B100, 136-141

Sharma, P., & Bhatti, H. (2009). Laser induced down conversion optical characterizations of synthesized $Zn_{2-x}Mn_xSiO_4$ ($0.5 \leq x \leq 5$ mol%) nanophosphors. Journal of Alloys and Compounds, 473, 483-489

Tabor, D. (2000). The Hardness of Metal. Oxford: Oxford University Press

Takesue, M., Hayashi, H., & Smith, R. L. (2009). Thermal and chemical methods for producing zinc silicate (willemite): A review. Progress in Crystal Growth and Characterization of Materials, 55, 98-124

Takesue, M., Suinob, A., Hakutab, Y., Hayashib, H., & Smith, R. L. (2010). Crystallization trigger of Mn-doped zinc silicate in supercritical water via Zn, Mn, Si sources and complex in agent ethylenediamine tetraacetic acid. Materials Chemistry and Physics , 121, 330-334

Tani, T., Takatori, K., & Pratsinis, S. E. (2004). Evolution of the Morphology of Zinc Oxide/Silica Particles by Spray Combustion. Journal of the American Ceramic Society, 87, 365-370

Tani, T., Watanabe, N., & Takatori, K. (2003). Emulsion combustion and flame spray synthesis of zinc oxide/silica particles. Journal of Nanoparticle Research, 5, 39-46

Williamson, G., & Hall, W. (1953). X-ray Line Broadening from Filed Aluminum and Wolfram. Acta Metallurgica, 1, 22-31

Xu, C., Sun, X., Dong, Z., Yu, M., My, T., Zhang, X., et al. (2004). Zinc oxide nanowires and nanorods fabricated by vapour-phase transport at low temperature. Nanotechnology, 15, 839-842

Xu, G., Xu, H., Zheng, Z., & Wu, Y. (2010). Preparation and characterization of Zn_2SiO_4: Mn phosphors with hydrothermal methods. Journal of Luminescence, 130, 1717-1720

Xu, J., O'Keefe, E., & Perry, C. C. (2004). The preparation and characterization of sol–gel zinc silicate glass particles with pyramid shape and millimetre size. Journal of Materials Chemistry, 14, 1774-1748

Yan, J., Ji, Z., Xi, J., Wang, C., Du, J., & Zhao, S. (2006). Fabrication and characterization of photoluminescent Mn-doped- Zn_2SiO_4 films deposited on silicon by pulsed laser deposition. Thin Solid Films, 515, 1877–1880

Ying-Mei, X., Ji, Q., De-Min, H., Dong-Mei, W., Hui-Ying, C., Jun, G., et al. (2010). Preparation of Amorphous Silica from Oil Shale Residue and Surface Modification by Silane Coupling Agent. Oil Shale, 27, 37-46

Zeng, J. H., Fu, H. L., Lou, T. J., Yu, Y., Sun, Y. H., & Li, D. Y. (2009). Precursor, base concentration and solvent behavior on the formation of zinc silicate. Materials Research Bulletin, 44, 1106-1110

Zhang, H., Buddhudu, S., Kam, C., Zhou, Y., Lam, Y., Wong, K., et al. (2001). Luminescence of Eu^{3+} and Tb^{3+} doped Zn_2SiO_4 nanometer powder phosphors. Materials Chemistry and Physics, 68, 31-35